

Preparation and characterization of SDS-stabilized hydrophobic porphyrinic nanoaggregates in water

L. Maqueira^{a,b,*}, A. Iribarren^b, A. C. Valdés^b, Celso P. de Melo^c and Clécio G. dos Santos^d

^a Departamento de Química Analítica, Facultad de Química, Universidad de La Habana, Zapata y G, Vedado, C.P. 10400, La Habana, Cuba

^b Instituto de Ciencia y Tecnología de Materiales, Universidad de La Habana, Zapata y G, Vedado, C.P. 10400, La Habana, Cuba

^c Departamento de Física, Universidade Federal de Pernambuco, 50670-901 Recife, PE Brazil

^d Pós-Graduação em Ciência de Materiais, Universidade Federal de Pernambuco, 50670-901 Recife, PE Brazil

Received 8 August 2011

Accepted 23 December 2011

ABSTRACT: Porphyrin nanoaggregates formed in the interior of colloidal suspensions can be considered as examples of supramolecular systems with self-organized architecture. Due to their peculiar optical and electrochemical properties such as decrease of fluorescence, increase of conductivity and possible electron transfer, these aggregates can be used in the design and fabrication of optoelectronic devices, such as organic solar cells and optical and electrochemical sensors. In this paper, we first describe the synthesis of a series of hydrophobic tetraphenylporphyrins by a change in the order of reagents addition that results in high yields of the desired products. These products were then employed to obtain stable suspensions of porphyrinic nanoaggregates in aqueous solutions of sodium dodecyl sulfate (SDS). The aggregates resulting of the encapsulation of the tetraphenylporphyrins into the micelles of the surfactant were studied by dynamic light scattering (DLS), atomic force microscopy (AFM) and UV-vis and fluorescence spectroscopies. The results indicate that the nanoaggregates have a spherical morphology with particles whose average size ranges between 46–78 nm and ζ -potential values (higher than 55 mV), indicative of excellent stability. Optical characterization was used to determine the classification of nanoaggregates, according to the observed shifts on the absorption spectra.

KEYWORDS: porphyrin, SDS, porphyrinic nanoaggregates.

INTRODUCTION

Porphyrins are excellent examples of the versatility of the supramolecular organic chemistry [1–4] because, as macrocycles of tetrapyrroles with a chemical structure of high conjugation and rigidity that can be obtained by well-established synthetic methods, they enable the creation of a large number of derivatives with diverse functionalities [5]. The remarkable photo-, catalytic-, electro-, and biochemical properties of porphyrins and

their metallo derivatives are well-described in the literature [6–9], and have been extensively exploited in the fabrication of a variety of devices such as solar cells [10–12] and optical and electrochemical sensors [13–15].

In fact, porphyrins present structural and chemical characteristics that favor self-assembly in different ways, by use of intermolecular H-bonding, π – π or electrostatic interactions and direct coordination to the central metal ion, and these particular properties have been extensively used to prepare self-assembled monolayers (SAM) and thin films and porphyrin nanoparticles (*i.e.* nanoscale aggregates) [5, 16, 17]. Those nanoaggregates can be prepared through the use of several methods, such as (1) the rapid exchange of solvent, (2) host/

*Correspondence to: Luis Maqueira, email: maqueira@fq.uh.cu, tel: +537 873-8222 and Augusto Iribarren, email: augusto@imre.oc.uh.cu, tel: +537 8781004/06 ext. 221

[†]Bolsista da CAPES

guest solvents whereby aggregation occurs by mixing of solutions containing porphyrins with miscible solvents in which they are not soluble (e.g. $\text{CHCl}_3/\text{H}_2\text{O}$) and stabilized by surfactants or amphipathic molecules, (3) interfacial precipitation, and (4) the rapid expansion of supercritical solvents [1]. Besides, porphyrin nanorods have been obtained by employing sonication [18].

In general terms, porphyrin aggregates could be of two types, depending on the order of the adopted molecular arrangement, *i.e.* H-aggregates, when the arrangement is face-to-face and J-aggregates if side-by-side (or edge-to-edge) [1]. The occurrence of these two types of aggregates could be in principle identified by optical spectroscopy, since the H-aggregates produce a blue shift in the Soret band whereas a red shift is observed if J-aggregates are present, both in comparison to the spectra of monomeric porphyrin [1, 19, 20]. Once formed, the aggregates can favor electron transfer in these supramolecular systems, leading to noticeable changes in the optical and electrochemical properties that contribute to extend the range of possible applications of these materials. For example, porphyrin-doped polymer films can be prospectively used in optoelectronics and sensor [21].

On the other hand, to obtain stable nanoaggregate suspensions of porphyrins in water is also relevant because of its possible use in biological applications photosensitizer in polymer/porphyrins complex with antibacterial activity [22]. However, the preparation of hydrophobic porphyrin suspensions could be difficult. Due to this it is necessary the search for new methods to obtain stable dispersions of hydrophobic porphyrins and metalloporphyrins in water [23].

In this work, a series of hydrophobic porphyrins and metalloporphyrins substituted by different functional groups was synthesized and used to obtain porphyrin nanoaggregates in water, through a novel method that allows the formation of highly stable hydrophobic porphyrinic nanoaggregates dispersed in an aqueous medium. The optical, morphological properties and the stability of these nanoaggregates suspensions were studied by dynamic light scattering (DLS), UV-vis and fluorescence spectroscopies and by atomic force microscopy (AFM).

EXPERIMENTAL

Equipments

The porphyrin aqueous microemulsions solutions were prepared by use of an ultrasonic probe (Ultrasonic Processor Sonics, Vibra.cell), with a regime of 130 watts power and 20 KHz frequency. Samples were treated with an Ultracentrifuge Hermle Z300.

UV-vis spectra were recorded by using a Varian Cary5E UV-vis/NIR spectrophotometer. Fluorescence measurement were carried out on an ISS Vinci Model PC1 spectrofluorimeter with excitation and emission

slits at 1 mm and lamp current at 15 A. Particles size and ζ -potential were measured by dynamic light scattering using a Zetasizer NanoSeries, Model Nano-ZS290 (Malvern Instruments). AFM images were recorded with a PicoScan 2500 (Molecular Imaging). Nuclear magnetic resonance (NMR) spectra were recorded on a Bruker 100-MHz (AMX 100) FT-NMR instrument and were carried out using CDCl_3 .

Materials

Propionic acid (Sigma-Aldrich, 99%), aldehydes (*o*-methoxybenzaldehyde, *o,p*-dimethoxybenzaldehyde and benzaldehyde (Sigma-Aldrich, 99%)) of analytical grade were used. Pyrrole (Sigma-Aldrich, 99%) was distilled prior to synthesis.

Synthesis of porphyrins and its metallic derivatives

Porphyrins were synthesized according to the procedure reported by Adler *et al.* [24], but with the modification in the order of reagents addition suggested by Ortega *et al.* [25] to increase the reaction yield (see Supporting information section).

Metallic derivatives were obtained by refluxing the corresponding metal acetate together with porphyrin in DMF for 20 min, with subsequent precipitation on cold water and vacuum filtering. All products were characterized by UV-vis, and the nonmetallic derivatives by NMR- ^1H and NMR ^{13}C . The corresponding structures of the synthesized porphyrins are presented in Table 1.

NMR ^1H and ^{13}C of nonmetallic porphyrins were carried out, and the corresponding results were:

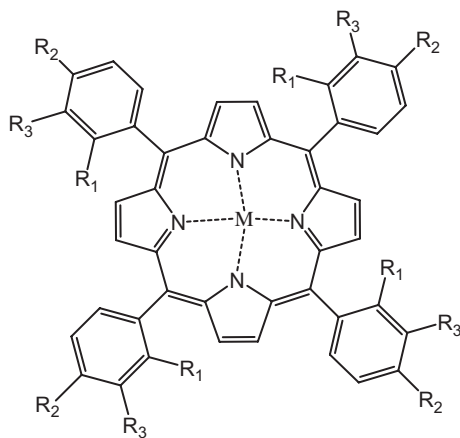
Tetraphenylporphyrin (TPP). In 20 mL of propionic acid 0.32 mL of pyrrole (5 mmol) and benzaldehyde (5 mmol) were added and refluxed by 1 hour. The obtained dark solid was vacuum filtered and dried to give 79% yield of TPP. ^1H NMR (CDCl_3): δ , ppm 8.89 (s, 8H, H β), 8.27–7.79 (m, 20H, H aromatics), -2.73 (s, 2H, NH). ^{13}C NMR (CDCl_3): δ , ppm 142.23 (C1), 134.63 (C2,6), \approx 131.3 (C β), 127.78 (C4), 126.76 (C3,5), 120.22 (C *meso*).

***o*-methoxy-tetraphenylporphyrin (OMTPP).** In 20 mL of propionic acid 0.32 mL of pyrrole (5 mmol) and *o*-methoxy-benzaldehyde (530 mg, 5 mmol) dissolved in 1 mL of propionic acid were added and refluxed by 1 h. The obtained dark solid was vacuum filtered and dried to give 56% yield of OMTPP. ^1H NMR (CDCl_3): δ , ppm 8.74 (s, 8H, H β), 8.01–7.25 (m, 20H, H aromatics), 3.56 (s, 3H, OCH $_3$), -2.60 (s, 2H, NH).

***o,p*-dimethoxy-tetraphenylporphyrin (OPMTPP).** In 20 mL of propionic acid 0.32 mL of pyrrole (5 mmol) and *o,p*-methoxy-benzaldehyde (681 mg, 5 mmol) dissolved in 1 mL of propionic acid were added and refluxed by 1 h. The obtained dark solid was vacuum filtered and dried to give 62% yield of OPMTPP. ^1H NMR (CDCl_3): δ , ppm 8.74 (s, 8H, H β), 7.94–6.87 (m, 20H, H aromatics), 3.55 (s, 3H, OCH $_3$), 3.52 (s, 3H, OCH $_3$), -2.66 (s, 2H, NH).

Table 1. Structures and abbreviation of the porphyrins synthesized

Abbreviation	R1	R2	R3	M
TPP	H	H	H	—
ZnTPP	H	H	H	Zn
CuTPP	H	H	H	Cu
OMTPP	-OCH ₃	H	H	—
OPMTPP	-OCH ₃	-OCH ₃	H	—



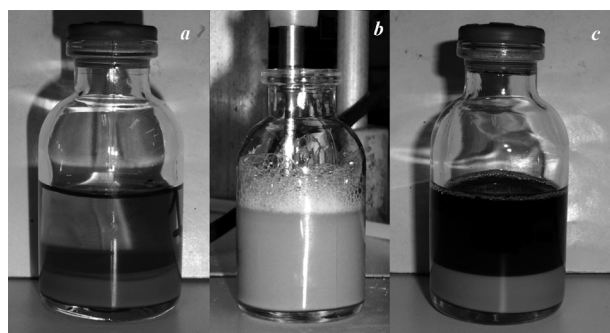
Preparation of hydrophobic porphyrin water dispersions stabilized with SDS

Hydrophobic porphyrinic dispersed in aqueous solutions were obtained using sodium dodecyl sulfate (SDS) as surfactant and after sonication. Initially a pre-emulsion of the porphyrin dissolved in chloroform and the SDS aqueous solution (0.1 g in 10 mL) was prepared and then stirred for about 1 h. Later, a microemulsion was obtained by ultrasonication of the pre-dispersion for 3 min at 70% amplitude. Finally, the material was rotoevaporated to remove the organic solvent, and centrifuged for 30 min at 10,000 rpm, and then filtered through a 0.22 μm membrane.

RESULTS AND DISCUSSION

Nanoaggregates suspension: particle size, morphology and stability

A stable suspension of porphyrins remained dispersed in the aqueous medium. Figure 1 shows the porphyrin dispersions before, during and after sonication. Figure 1(a) shows the pre-emulsion obtained after magnetic stirring, but before sonication, where the clear layer corresponds to a few porphyrin encapsulated


Fig. 1. Pictures of porphyrinic dispersions ($\text{CHCl}_3/\text{SDS}/\text{H}_2\text{O}$), before (a) during (b) and after (c) sonication

into the surfactant (SDS) dispersed in water, whereas the greyish layer is the mixing between water, SDS and porphyrin dissolved in chloroform. Later, this pre-emulsion is sonicated (Fig. 1(b)) to obtain a stable suspension of porphyrin nanoaggregates in water, which is the dark layer in Fig. 1(c), where the greyish layer is the unstable layer produced. Afterwards, this unstable layer fully disappears after a rotoevaporating step for eliminating chloroform from the suspension.

Although a similar method has been reported to produce nanoparticles of water-soluble polymers [26], to our knowledge, this procedure had not been used before for the preparation of porphyrin nanoaggregates. In fact, the method here adopted can be considered as a combination of two other procedures independently used for the preparation of porphyrinic nanoaggregates: while one of them, employs surfactants, the other one uses sonication with ultrasonic bath [1, 18]. In our case, the use of ultrasonic probe guarantees the full introduction of the dissolved porphyrin in the interior of the SDS micelles, a factor that leads to highly stable suspensions.

To examine the stability of each suspension, we have measured the average size of the dispersed particles and their ζ -potential by DLS, and the corresponding results are shown in Table 2, where the full width at half maximum (fwhm) values are also shown. Figure 2 exemplifies the size distribution with that of ZnTPP

Table 2. Particle size and ζ -potential of water-dispersed porphyrins

Porphyrins	d, nm	fwhm, nm	ζ -potential, mV
TPP	64	62	-55.9
ZnTPP	65	41	-70.1
CuTPP	59	53	-68.9
OMTPP	78	55	-70.9
OPMTPP	46	54	-73.6

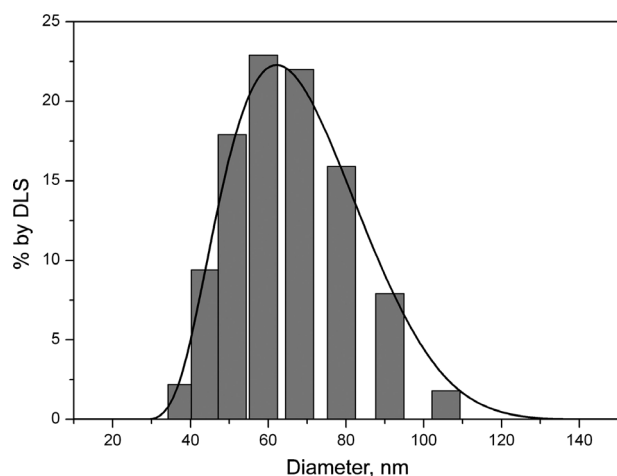


Fig. 2. DLS characterization of ZnTPP nanoaggregates, mean diameter = 65 nm

nanoaggregate, where it is noticed the distribution skewed shape. A similar shape of distribution was obtained for all porphyrin nanoaggregates. See the supporting information for results of DLS characterization of the other studied porphyrins.

In general, average particle sizes for each porphyrin change between 46 nm and 78 nm. Fwhm values indicate relatively high dispersion in comparison to other reports [16], where ZnTPP distribution was the narrowest one. However, in all cases, the absolute value of the measured ζ -potential of the suspended particles was higher than 50 mV, in an indication that the corresponding colloidal solutions presented a high stability. As it should be expected, these ζ -potentials had negative values because the negatively charged dodecylsulphate ions form the most external shell of the aggregates.

On the other hand, morphological studies of the TPP nanoaggregates by AFM, employing the drop dispersed method to prepared sample. AFM images reveal spherical particles with size ranging between 50 nm and 90 nm, as shown in Fig. 3.

Characterization of porphyrin nanoaggregates in water by UV-vis and fluorescence

In general, porphyrins have very strong absorption bands around 400–450 nm (Soret band) with an extinction molar coefficient (ϵ) of about $10^5 \text{ M}^{-1}\cdot\text{cm}^{-1}$ and four Q-bands between 500 and 700 nm with values of ϵ 10–20 times lower. Their metallo-derivatives present only one or two Q-bands with similar ϵ , depending on the metal [1]. The UV-visible spectrum of each nanoaggregate suspension in water were recorded and compared with those obtained with chloroform-dissolved porphyrins (see supporting information). In order to establish such comparison, all samples were adjusted to the same concentration value. In Table 3, the Soret and Q-bands of porphyrin dispersed in chloroform and water, respectively, are presented. All spectra of water-dispersed porphyrins showed that the Soret band broadens and the absorbance decreases in comparison to non-aggregated porphyrins in chloroform (see Supporting information section). In general, no significant shifts were observed from the region, and so it was not possible to assign them as J- or H-aggregates [5, 19].

However, in the case of the metallic derivatives one could observe the existence of small red shifts, which were more significant in the Zn substituted porphyrin, (see Fig. 4); a fact suggestive of the presence of J-type aggregate [1]. On the other hand, in the case of non-metal porphyrins, only the methoxyl disubstituted porphyrins were the ones to present some variation on absorption spectra, with blue-shifts — characteristic of the existence of H-type aggregates — on the Soret band.

In Table 4 one can note the shift of the emission bands of water-dispersed ZnTPP, which is in agreement with the result obtained in the absorption spectrum of this porphyrin. The methoxylated products show increases in the emission intensity when compared to non-functionalized porphyrins, because this functional group produces a positive mesomeric effect on the porphyrin ring, increasing the average electron density and the transition $\pi-\pi^*$ [27].

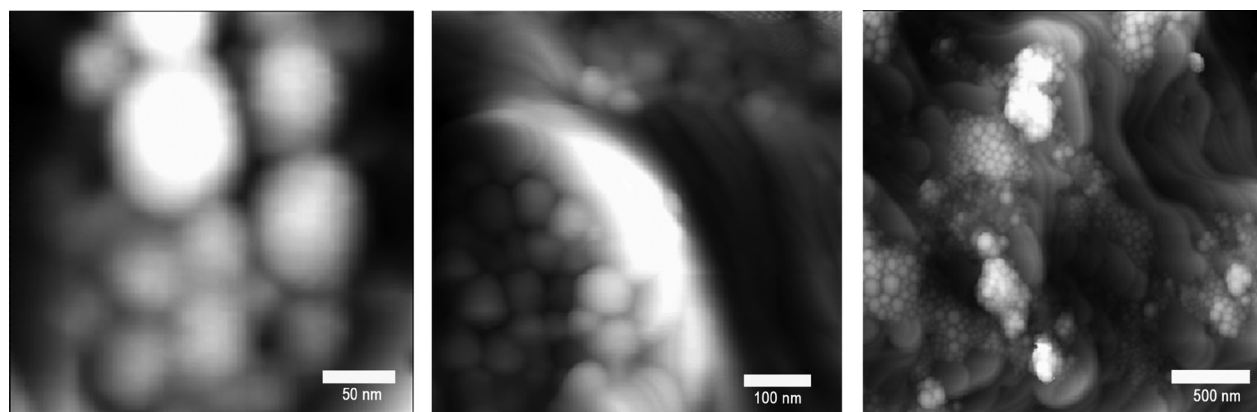


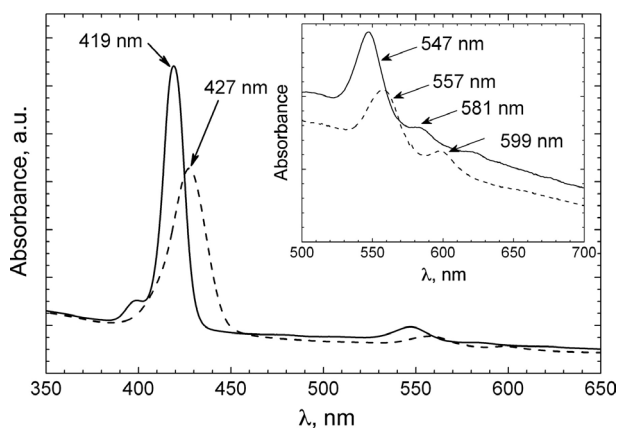
Fig. 3. Morphology of porphyrin nanoaggregates as revealed by AFM

Table 3. Comparison of the absorption band maxima between water-suspended nanoaggregates and chloroform-dissolved non-aggregate porphyrins (in nm)

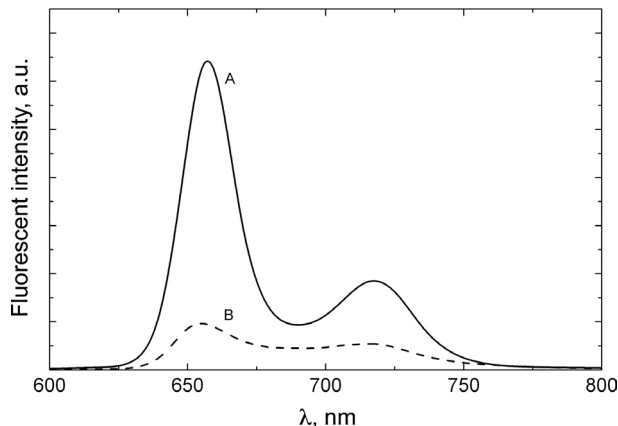
Porphyrins	Porphyrins in CHCl ₃					Porphyrins in H ₂ O				
	Soret band		Q-bands			Soret band		Q-bands		
TPP	418	515	549	588	646	419	517	549	590	646
ZnTPP	419	547	581	—	—	427	557	599	—	—
CuTPP	416	538	—	—	—	415	540	—	—	—
OMTPP	419	515	549	590	652	421	515	551	591	652
OPMTPP	422	516	550	592	651	417	517	552	590	646

Table 4. Emission wavelength of porphyrin in organic and aqueous media (in nm)

Porphyrins	Porphyrins in CHCl ₃		Porphyrins in H ₂ O	
	$\lambda_{\text{emission}}(1)$	$\lambda_{\text{emission}}(2)$	$\lambda_{\text{emission}}(1)$	$\lambda_{\text{emission}}(2)$
TPP	653	715	654	715
ZnTPP	597	645	603	654
OMTPP	655	715	655	715
OPMTPP	653	715	654	715


Fig. 4. Absorption spectra of ZnTPP (solid line) and ZnTPP nanoaggregate (dashed line)

Fluorescence signals in the 600–800 nm region were not observed for Cu porphyrin, in agreement with previous reports [27]. The fluorescence spectra of the water-dispersed nanoaggregates and chloroform-dissolved porphyrins are compared in Fig. 5. In order to attain such comparison, the same concentration ($c = 1.58 \times 10^{-5}$ M) and similar instrumental conditions were used in all cases. The fluorescence intensity in water-suspended porphyrins decreases in comparison to those of the chloroform-dissolved ones. Porphyrin nanoaggregates usually present a quenching of the fluorescence due to several factors, such as non-radiative pathways and photoscreening of chromophores. Particles with sizes lower than 150 nm are reported to present anomalous and depressed fluorescence [5] (see Supporting information section).


Fig. 5. Fluorescence spectra of OPMTPP water-suspensions (A) and OPMTPP in CHCl₃-dissolved (B), $c = 1.58 \times 10^{-5}$ M and excited at 420 nm in both case

CONCLUSIONS AND PERSPECTIVES

We have developed a simple modified procedure for preparation of porphyrin nanoaggregates that allowed us to obtain aqueous suspensions of hydrophobic porphyrins with excellent colloidal stability. DLS and AFM measurements showed that the aggregates exhibit spherical morphology and are nanostructured. UV-vis and fluorescence spectroscopic characterization has permitted us to discern the dispersed porphyrin particles in suspension as of J- or H-type nanoaggregates.

Recently, the light harvesting properties of conducting polymers have been exploited in the design of (conjugated polymers)/porphyrin complexes that could be used in the detection of heavy metals ions [28] or as light-activated antibacterial agents [22]. It would be of special interest to examine the equivalent properties of complexes formed by water-soluble conjugated polymers and the porphyrin derivatives described in the present work.

Acknowledgements

This work was partially supported by Project 040/07 CAPES, Brasil – MES, Cuba and it is also under Project PNCIT-DES 00613457.

Supporting information

The results of UV-visible absorption spectra, fluorescent spectra and DLS characterization of porphyrins nanoaggregates are given in the supplementary material. This material is available free of charge via the Internet at <http://www.worldscinet.com/jpp/jpp.shtml>.

REFERENCES

1. Drain CM, Varotto A and Radivojevic I. *Chem. Rev.* 2009; **109**: 1630–1658.
2. Mohnani S and Bonifazi D. *Coord. Chem. Rev.* 2010; **254**: 2342–2362.
3. Schmittel M, He B and Mal P. *Org. Lett.* 2008; **10**: 2513–2516.
4. Jurow M, Schuckman AE, Batteas JD and Drain CM. *Coord. Chem. Rev.* 2010; **254**: 2297–2310.
5. Drain CM, Smeureanu G, Patel S, Gong XC, Garno J and Arijeloye J. *New J. Chem.* 2006; **30**: 1834–1843.
6. Chen W, Wang Y, Bruckner C, Li CM and Lei Y. *Sens. Actuators, B* 2010; **147**: 191–197.
7. Mazzotta E and Malitesta C. *Sens. Actuators, B* 2010; **148**: 186–194.
8. Bai D, Wang Q, Song Y, Li B and Jing H. *Catal. Commun.* 2011; **12**: 684–688.
9. Rezaeifard A, Jafarpour M, Raissi H, Ghiamati E and Tootoonchi A. *Polyhedron* 2011; **30**: 592–598.
10. Kim H-S, Kim C-H, Ha C-S and Lee J-K. *Synth. Met.* 2001; **117**: 289–291.
11. Watson DF, Hasselmann GM and Meyer GJ. “NCPV and Solar Program Review Meeting” 2003.
12. Maree CHM, Roosendaal SJ, Savenije TJ, Schropp REI, Schaafsma TJ and Habraken F. *J. Appl. Phys.* 1996; **80**: 3381–3389.
13. D’Souza F, Hsieh Y-Y, Wickman H and Kutner W. *Chem. Commun.* 1997: 1191–1192.
14. Deviprasad GR, Keshavan B and D’Souza F. *J. Chem. Soc., Perkin Trans. 1* 1998: 3133–3135.
15. Rakow NA, Sen A, Janzen MC, Ponder JB and Suslick KS. *Angew. Chem., Int. Ed.* 2005; **44**: 4528–4532.
16. Gong X, Milic T, Xu C, Batteas JD and Drain CM. *J. Am. Chem. Soc.* 2002; **124**: 14290–14291.
17. Bazzan G, Smith W, Francesconi LC and Drain CM. *Langmuir* 2008; **24**: 3244–3249.
18. Hasobe T, Oki H, Sandanayaka ASD and Murata H. *Chem. Commun.* 2008: 724–726.
19. Maiti NC, Mazumdar S and Periasamy N. *J. Phys. Chem. B* 1998; **102**: 1528–1538.
20. Barber DC, Freitagbeeston RA and Whitten DG. *J. Phys. Chem. B* 1991; **95**: 4074–4086.
21. Egawa Y, Hayashida R and Anzai JI. *Langmuir* 2007; **23**: 13146–13150.
22. Xing CF, Xu QL, Tang HW, Liu LB and Wang S. *J. Am. Chem. Soc.* 2009; **131**: 13117–13124.
23. Chen C-Y, Tian Y, Cheng Y-J, Young AC, Ka J-W and Jen AKY. *J. Am. Chem. Soc.* 2007; **129**: 7220–7221.
24. Adler AD, Longo FR, Finarell. Jd, Goldmach J, Assour J and Korsakof L. *J. Org. Chem.* 1967; **32**: 476-&.
25. León-Cedeño F, Menes-Arzate M and García-Ortega H. *Rev. Cubana Quí.* 2006; **XVIII**.
26. Kietzke T, Neher D, Landfester K, Montenegro R, Guntner R and Scherf U. *Nat. Mater.* 2003; **2**: 408–U407.
27. Zheng WQ, Shan N, Yu LX and Wang XQ. *Dyes Pigm.* 2008; **77**: 153–157.
28. Fang Z, Pu KY and Liu B. *Macromolecules* 2008; **41**: 8380–8387.